

See discussions, stats, and author profiles for this publication at: <https://www.researchgate.net/publication/7671796>

Force Spectroscopy of Quadruple H-Bonded Dimers by AFM: Dynamic Bond Rupture and Molecular Time–Temperature Superposition

ARTICLE *in* JOURNAL OF THE AMERICAN CHEMICAL SOCIETY · AUGUST 2005

Impact Factor: 12.11 · DOI: 10.1021/ja0531475 · Source: PubMed

CITATIONS

59

READS

37

3 AUTHORS:



Shan Zou

National Research Council Canada

59 PUBLICATIONS 1,339 CITATIONS

SEE PROFILE



Holger Schönherr

Universität Siegen

202 PUBLICATIONS 4,897 CITATIONS

SEE PROFILE



Gyula Julius Vancso

University of Twente

277 PUBLICATIONS 6,454 CITATIONS

SEE PROFILE

Force Spectroscopy of Quadruple H-Bonded Dimers by AFM: Dynamic Bond Rupture and Molecular Time–Temperature Superposition

Shan Zou, Holger Schönherr, and G. Julius Vancso*

Materials Science and Technology of Polymers, MESA⁺ Institute for Nanotechnology, University of Twente, 7500 AE Enschede, The Netherlands

Received May 13, 2005; E-mail: g.j.vancso@utwente.nl

Noncovalent molecular interactions govern the formation of well-defined, hierarchical (supra)molecular architectures in spontaneous self-assembly processes.^{1–3} The strength of these molecular interactions has traditionally been assessed by ensemble thermodynamics.⁴ However, with the growing interest in molecular level biochemistry and -physics, as well as molecular nanotechnology, there is an increasing need for knowledge regarding molecular stability and bond strengths from the single-molecule perspective, i.e., without ensemble averaging. Atomic force microscopy (AFM) allows one to obtain data on bond rupture and molecular force–stretching behavior of biological and synthetic macromolecules in single-molecule force spectroscopy (SMFS)⁵ measurements. In these experiments the imaging media (solvents) and temperature as well as the linkage stiffness (cantilever spring constant, polymer spacer) and loading rates can, in principle, be varied. First insights into the theory of dynamic SMFS and rupture forces have been provided by Evans and co-workers⁶ based on earlier models by Bell.⁷ Related theories, e.g., by Hummer and Szabo, have been the subject of continuing interest.⁸ While the rupture forces depend logarithmically on the loading rate in far from equilibrium conditions according to Evans et al.,⁶ quasi-equilibrium conditions lead to loading-rate independent rupture forces, as confirmed by several studies.⁹

The accessible loading-rate range (using commercial AFMs and varying only the piezo retraction rate) stretches over ca. 3.5 decades, which is rather limited. The objective of this communication is to demonstrate the utility of the time–temperature superposition principle on the molecular scale for single-molecule rupture-force studies, which allows one to significantly broaden this range. Central to this approach are SMFS experiments, which are carried out at different temperatures to vary the complexation constant, K_{eq} , and the bond lifetime in a controlled way. The data form the basis for the construction of force–loading rate master curves.

The approach is demonstrated for the well-known quadruple H-bonded ureido-4[1H]-pyrimidinone (UPy) system. Owing to their strong self-complementary interactions in apolar solvents, UPy moieties form the basis of a wide range of reversible supramolecular polymers, which exhibit tunable properties via the variation in complex stability (i.e., average bond lifetime) as a function of temperature and/or solvent composition.³ Here we report on measurements of single-molecule unbinding forces of dimeric (UPy)₂ complexes under dynamic loading conditions covering thermodynamic quasi-equilibrium (loading-rate independence), the transition from quasi-equilibrium to nonequilibrium, and the nonequilibrium (loading-rate dependent) domain by variable-temperature SMFS in organic media.

Our SMFS studies are based on a previously developed self-assembled monolayer (SAM) platform on Au comprising poly-(ethylene glycol) (PEG)-linked UPy disulfides (Figure 1A).^{10,11} The PEG spacer efficiently decouples the complexation process from the surface and hence suppresses contributions resulting from

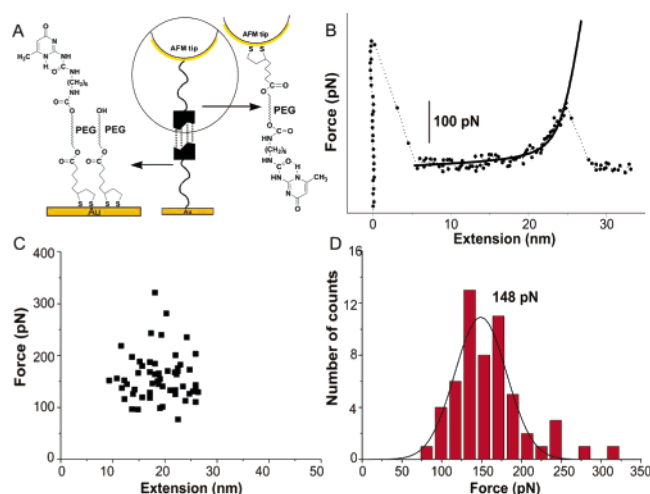


Figure 1. (A) Scheme of PEG–UPy disulfide self-assembled both on Au-coated AFM tip and Au substrate. (B) Representative *f*–*e* curve measured between PEG–(UPy)₂ complexes by SMFS ($r_f = 5.7 \pm 1.1$ nN/s; $T = 301$ K; HD). The fit of the data to the modified freely jointed chain model (Kuhn segment length 0.76 ± 0.06 nm, segment elasticity 6.3 ± 0.7 nN/nm)¹⁰ is shown as a solid line. (C) Rupture forces vs corresponding rupture lengths of (UPy)₂ complexes. (D) Histogram of rupture forces of individual (UPy)₂ complexes (solid line: Gaussian fit).

secondary interactions and, in addition, allows one to unequivocally identify single-molecule stretching and, thus, bond-rupture events.¹²

Our earlier SMFS measurements in hexadecane (HD) yielded the rupture force of single (UPy)₂ complexes of 180 ± 21 pN ($T = 301$ K, fixed loading rate $r_f = 35$ nN/s).¹⁰ Given the high complexation constant of UPy in HD (K_{eq} of $\sim 10^9$ M^{−1}),¹³ the rupture forces are expected to be loading-rate dependent under these conditions.⁶

A typical force–extension (*f*–*e*) curve measured between PEG–(UPy)₂ complexes at 301 K in HD for a rate of 5.7 ± 1.1 nN/s, including the rupture of the quadruple H-bond array, is shown in Figure 1B. Prior to (UPy)₂ rupture the spacer (ca. 12 nm length)¹⁰ must be fully stretched, hence only rupture events with rupture lengths between 11 and 25 nm, corresponding to two spacers, were considered for the analysis. The observed stretching events in *f*–*e* curves are attributed to the stretching of single PEG spacers (based on the fitted Kuhn length and segment elasticity values).¹⁰ The value of the mean rupture force (148 pN) was significantly lower than that reported previously for a rate of 35 nN/s, consistent with the anticipated loading-rate dependence.

The systematic determination of the rupture forces at 301 K was carried out for loading rates between ~ 5 nN/s and ~ 500 nN/s (see also Supporting Information Figure S1). As shown in Figure 2A, the rupture forces at 301 K were found to depend logarithmically on the loading rate, consistent with the prediction by Evans et al.⁶ describing the most probable rupture force f^* : $f^* = f_\beta$

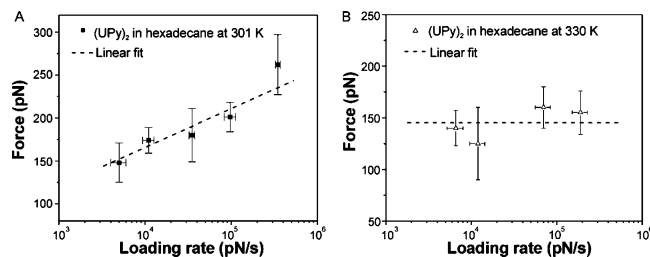


Figure 2. Plot of rupture force of (UPy)₂ complexes vs loading rate at (A) 301 K and (B) 330 K in HD.

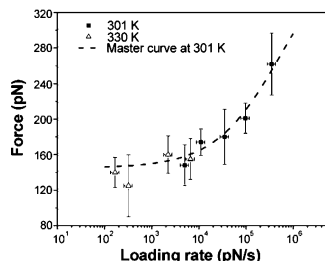


Figure 3. Master plot of crossover from loading-rate independence to loading-rate dependence of rupture forces of single (UPy)₂ complexes in HD at $T_{\text{ref}} = 301$ K (the dashed line serves to guide the eye).

$\ln(r_f/r_f^0)$, where the thermal activation introduces the characteristic force scale f_β , and a thermal scale for loading rate $r_f^0 = f_\beta/t_{\text{off}}(0)$ ($t_{\text{off}}(0)$ denotes the complex lifetime at zero force, f_β corresponds to the slope of the f^* vs $\log r_f$ plot). The observed dependence with a slope f_β of ~ 19 pN indicates that the SMFS measurements (at 301 K in HD) are carried out under thermodynamic *nonequilibrium* conditions.

By contrast, for measurements carried out in situ at 330 K using a custom-built heating device, no loading-rate dependence was observed for rates between 5 nN/s and 200 nN/s (Figure 2B; see also Supporting Information, Figure S2). This observation indicates that the corresponding experiment was carried out under *quasi-equilibrium* conditions.⁹ Assuming that (a) K_{eq} decreases 10 times in HD and that (b) the dissociation rate constant increases 50 times,^{13,14} when the temperature is changed from 301 to 330 K, it can be shown that the rupture forces at 330 K will depend on the loading rate only for values exceeding 300 nN/s (eq 1). This prediction is fully supported by our observations.

On the basis of the time–temperature superposition principle¹⁵ and the knowledge of the temperature dependence of K_{eq} , the two dynamic rupture-force spectra can be combined and plotted in one “master curve” at the reference temperature (T_{ref}) of 301 K (Figure 3). Central to the master curve construction is performing SMFS experiments at different temperatures to vary (in a controlled fashion) the complexation constant (and the bond lifetime). We then make use of the equivalence principle between time (frequency or rate) and temperature concerning molecular rearrangements known from, e.g., polymers.¹⁵ The construction of a master curve showing all loading rates at a chosen T_{ref} requires shifting of loading rate values to T_{ref} . For (UPy)₂ the change in the value of the crossover force^{6b} is negligible, when T is increased from 301 to 330 K. By using the equality between the calculated crossover force for 301 K and the loading-rate independent f^* observed at 330 K, the conversion formula can be easily calculated. This formula expresses values of $r_f^{301\text{ K}}$ as a function of $r_f^{330\text{ K}}$ and of the lifetime of the given bond t_{off} at the experimental temperatures (for the formula see ref 16). The values of the lifetimes (reciprocal rate constants for dissociation) are taken from the literature.^{13,14} The magnitude of shifting of the loading-rate axis was calculated as described, which allowed us to combine A and B of Figure 2 into

one master curve at the chosen T_{ref} of 301 K. The result, plotted in Figure 3, shows the rupture force as a function of the loading rate at the chosen T_{ref} covering six decades for the loading rate. The crossover force (from loading-rate independent to dependent regimes) can now be observed at ~ 145 pN (at $r_f \approx 5.6$ nN/s).

The time–temperature superposition approach described above (as worked out for one potential energy barrier) allows one to substantially extend the limited range of the experimentally accessible loading rates *without* changing the linkage stiffness. Thus, supramolecular interaction forces can be obtained over a wide range of loading rates in AFM-based SMFS experiments by controlling the temperature of the medium and calculating the loading-rate shift factor using the bond lifetime data at the experimental temperatures.

In summary, using SMFS, the unbinding of supramolecular quadruple hydrogen bonding (UPy)₂ complexes was directly probed in quasi-equilibrium and nonequilibrium states in situ by controlling the temperature. A single master curve for the rupture force was determined at a reference temperature using AFM-SMFS data obtained at different temperatures by applying the time–temperature superposition principle to molecular-scale rupture force experiments.

Acknowledgment. The authors acknowledge Iván J. Vera Marín for his contributions in designing the heating device for the AFM liquid cell. This work has been supported by the MESA⁺ Institute for Nanotechnology of the University of Twente.

Supporting Information Available: Additional data (histograms of rupture forces) and experimental details. This material is available free of charge via the Internet at <http://pubs.acs.org>.

References

- (1) Lehn, J. M. *Supramolecular Chemistry: Concepts and Perspectives*; John Wiley & Sons: New York, 1995.
- (2) Reinhoudt, D. N.; Crego-Calama, M. *Science* **2002**, *295*, 2403–2407.
- (3) Sijbesma, R. P.; Beijer, F. H.; Brunsveld, L.; Folmer, B. J. B.; Hirschberg, J. H. K. K.; Lange, R. F. M.; Lowe, J. K. L.; Meijer, E. W. *Science* **1997**, *278*, 1601–1604.
- (4) Israelachvili, J. N. *Intermolecular and Surface Forces*; 2nd ed.; Academic Press: London, 1991.
- (5) For recent reviews, see: (a) Janshoff, A.; Neitzert, M.; Oberdorfer, Y.; Fuchs, H. *Angew. Chem., Int. Ed.* **2000**, *39*, 3213–3237. (b) Zhang, W.; Zhang, X. *Prog. Polym. Sci.* **2003**, *28*, 1271–1295.
- (6) (a) Merkel, R.; Nassoy, P.; Leung, A.; Ritchie, K.; Evans, E. *Nature* **1999**, *397*, 50–53. (b) Evans, E. *Annu. Rev. Biophys. Biomol. Struct.* **2001**, *30*, 105–128.
- (7) Bell, G. I. *Science* **1978**, *200*, 618–627.
- (8) Hummer, G.; Szabo, A. *Biophys. J.* **2003**, *85*, 5–15.
- (9) (a) Schönherr, H.; Beulen, M. W. J.; Bügler, J.; Huskens, J.; van Veggel, F. C. J. M.; Reinhoudt, D. N.; Vancso, G. J. *J. Am. Chem. Soc.* **2000**, *122*, 4963–4967. (b) Zapotoczny, S.; Auletta, T.; de Jong, M. R.; Schönherr, H.; Huskens, J.; van Veggel, F. C. J. M.; Reinhoudt, D. N.; Vancso, G. J. *Langmuir* **2002**, *18*, 6988–6994. (c) Auletta, T.; de Jong, M. R.; Mulder, A.; van Veggel, F. C. J. M.; Huskens, J.; Reinhoudt, D. N.; Zou, S.; Zapotoczny, S.; Schönherr, H.; Vancso, G. J.; Kuipers, L. J. *Am. Chem. Soc.* **2004**, *126*, 1577–1584.
- (10) Zou, S.; Schönherr, H.; Vancso, G. J. *Angew. Chem., Int. Ed.* **2005**, *44*, 956–959.
- (11) Zou, S.; Zhang, Z. H.; Förch, R.; Knoll, W.; Schönherr, H.; Vancso, G. J. *Langmuir* **2003**, *19*, 8618–8621.
- (12) Hinterdorfer, P.; Kienberger, F.; Raab, A.; Gruber, H. J.; Baumgartner, W.; Kada, G.; Riener, C.; Wielert-Badt, S.; Borken, C.; Schindler, H. *Single Mol.* **2000**, *1*, 99–103.
- (13) ten Cate, A. T.; Sijbesma, R. P. *Macromol. Rapid Commun.* **2002**, *23*, 1094–1112.
- (14) Sontjens, S. H. M.; Sijbesma, R. P.; van Genderen, M. H. P.; Meijer, E. W. *J. Am. Chem. Soc.* **2000**, *122*, 7487–7493.
- (15) Bird, R. B.; Curtiss, C. F.; Armstrong, R. C.; Hassager, O. *Dynamics of Polymer Liquids*; Wiley: New York, 1987.
- (16) $r_f^{T_1} = \frac{k_B T_1}{r_f^{T_2} t_{\text{off}}^{x_\beta}} \exp\left(\frac{T_2}{T_1} \ln\left(\frac{r_f^{T_2} t_{\text{off}}^{x_\beta}}{k_B T_2}\right)\right)$ with $T_1 = 301$ K, $T_2 = 330$ K; x_β is defined as: $f_\beta = k_B T/x_\beta$.

JA0531475